DYNAMICS OF THE DEVELOPMENT OF HIGH-CURRENT INDUCTION DISCHARGE

P. N. Baronets, V. I. Myshenkov, and M. I. Yakushin

UDC 533.92:621.039.01

1. Pulsed high-current discharges in the range of relatively low pressures were investigated mostly in connection with the problem of controlled thermonuclear fusion. The need for investigating such discharges at elevated pressures was dictated to a considerable extent by the requirement for high-power light sources. Significant advances in investigating the structure and dynamics of the development of high-current discharges have now been achieved. [1]. However, there also remain unsolved problems. In particular, with regard to pulsed induction discharges, complete understanding of the mechanism of development of such discharges is still lacking. Our purpose is to investigate high-current induction discharges in argon under gas pressures in the range from 5 to 50 mm Hg. A physical interpretation of individual stages in the development of high-current discharges is given on the basis of an analysis of the experimental results, and the stages of discharge development, the mechanism of which is not yet fully understood, are discussed. The discharge is investigated for relatively low energy inputs, when it is possible to separate in time the various stages of discharge development, which occur virtually simultaneously at high energy inputs.

2. The schematic diagram of the experimental device is shown in Fig. 1, where DT is a quartz tube with an inside diameter of ≈5 cm, where the discharge is produced, L is an inductor consisting of five turns, whose inductance is equal to ~5 μH, C is a capacitor bank, which can be charged to 25 kV, SG is the spark gap, PS is the pulse source (ÉV-45), SPR is a superhigh-speed photorecorder (SFR-2M), and CU is the control unit.

According to measurements performed by means of a Rogowski loop, the initial current amplitude in the inductor reaches 80 kA, while the frequency of current oscillations is equal to ~20 kHz. The initial amplitude of the discharge-maintaining rotational electric field near the walls of the discharge tube is equal to ~70 V/cm (only the azimuthal component of the rotational electric field, which is the most important one for maintaining the discharge in question, is contemplated throughout this article). The oscillograms of the strength E of the rotational electric field within the inductor in the zone adjacent to the discharge tube walls and of the electric current i through the inductor are shown on a relative scale in Fig. 2 from the time of breakdown initiation in the gas. The damping of the electric field and the current is connected with the electromagnetic energy loss in the form of Joule heat. Since, under our experimental conditions, the discharge current is considerably smaller (by one order of magnitude) than the current intensity in the inductor, the strength of the rotational electric field inside the inductor in discharge excitation has a phase shift of ≈90° with respect to the current i, as is the case in the absence of a discharge. The discharge is initiated by means of a grounded metal rod, which is introduced in the discharge tube. The discharge development is photographed at a rate of 2,500,000 frames/sec.

An analysis of the photographs obtained shows that, during the first quarter-period of current oscillations in the inductor (the time interval from 0 to $\tau/4$ in Fig. 2), there is weak ring-shaped gas luminescence (the photograph of this discharge stage is not shown). However, immediately following the breakdown, the discharge is not yet fully developed by the time the strength of the rotational field has diminished appreciably.

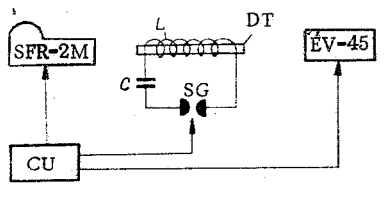

Fig. 1

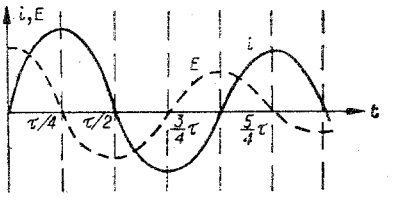

Fig. 2

Moscow. Translated from Zhurnal Prikladnoi Mekhaniki i Tekhnicheskoi Fiziki, No. 3, pp. 58-67, May-June, 1979. Original article submitted May 5, 1978.

0021-8944/79/2003-0305$07.50

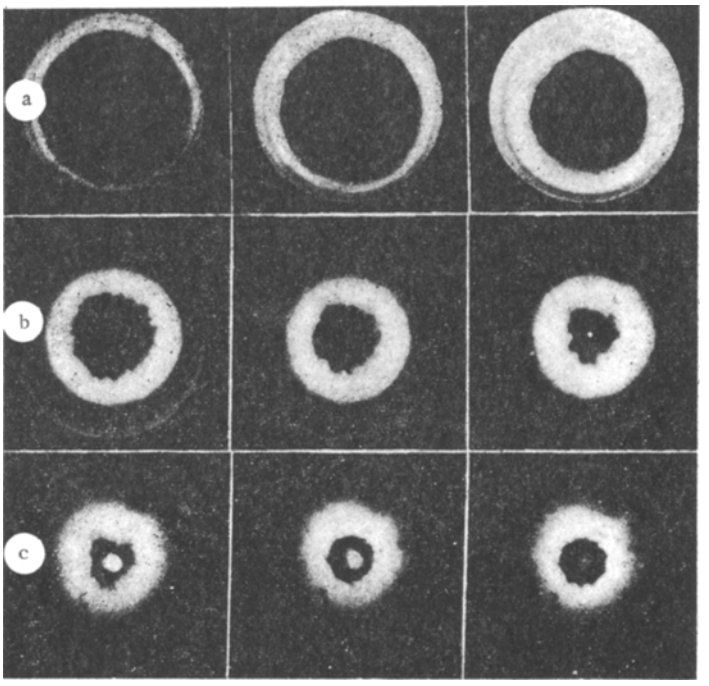

Fig. 3

During the next half-period (the time interval from $\tau/4$ to $3\tau/4$ in Fig. 2), there occurs a new, stronger breakdown (the time interval between the frames is equal to $1.5 \cdot 10^{-6}$ sec in Fig. 3), which has been facilitated by the preceding discharge. During the first few microseconds following the second breakdown, we observe a "swelling" of the discharge, which has the shape of a luminous ring. The "swelling" occurs at a rate of ~1 km/sec due to the movement of the inner discharge front in the direction of the tube axis (Fig. 3a). This is followed by sharp separation of the discharge from the tube walls. After a few microseconds, a bright plasmoid is formed inside the discharge ring at the tube axis (Fig. 3b). The plasmoid now gradually expands and starts to decay. As the strength of the rotational electric field diminishes, the plasma decays also in the discharge ring (Fig. 3c), which is accompanied by a blurring of the inner and outer discharge fronts. During the next half-period of current oscillations (the time interval from $(3/4)\tau$ to $(5/4)\tau$ in Fig. 2), the process is repeated; this occurs several times until the inductor current is greatly reduced.

The temperature is measured in the same way as in [2], using the method where probing radiation from an ÉV-45 pulse source at the 5500-Å wavelength is absorbed in the plasma. Measurements have shown that the plasma temperature in the discharge ring is equal to ≈10,000°K.

The following physical interpretation of the results can be given. The relatively low temperatures at the level of the specific power supplied to the discharge $\sigma E^2 \sim 200$ kW/cm^3 (σ is the conductivity) are explained by the fact that the plasma cannot be heated to higher temperatures during the development discharge. The above interpretation is supported by estimates. Therefore, in order to raise the discharge temperature, it is necessary to increase the gas heating rate, i.e., the strength of the electric field that maintains the discharge.

As is known, the abrupt separation of the discharge from the tube walls occurs under the action of electrodynamic forces (θ pinch effect). At the initial stage, immediately after the second gas breakdown, the pinch effect does not manifest itself because of the small value of the electrodynamic force.

The formation of the plasmoid at the center of the tube is caused by the action of a cylindrical shock wave, which, after cumulation at the axis, begins to propagate in the opposite direction. The existence of the shock wave was confirmed by an experiment performed with a hollow brass rod. The rod, fastened at the tube axis, was crumpled after every discharge.

In connection with the formation of a shock wave under the above conditions, the question arises concerning the mechanism of its development. We can indicate two processes leading to the development of a shock wave, which are separated from each other in space as well as in time. The first of them is connected with the vigorous energy release at the breakdown stage of discharge development and the subsequent supersonic expansion of heated gas, while the other is connected with the sharp action of electrodynamic forces on

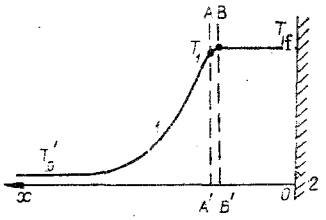

Fig. 4

the discharge as it separates from the tube walls. A detailed study of the development mechanism and the structure of the shock waves arising at various stages of the process would be of undoubted interest. However, this would require a theoretical consideration of this phenomenon and the results of special experiments, all of which are lacking at present.

There is also a lack of complete understanding of the mechanism of development of the initial stage of breakdown during the first quarter of the oscillation period of the inductor current (see Fig. 2), when the discharge is initiated. We can only assume that an ionization wave is formed as a result of the spark discharge between the high-voltage inductor turn and the grounded metal rod introduced in the discharge tube. As a result of the diffusion of resonance quanta [3], this wave spreads mostly over the region of maximum strength of the rotational electric field, i.e., along the walls of the discharge tube, which, in the final analysis, brings about the weak luminescence observed at this stage.

3. It would be of great interest to provide an explanation of the propagation mechanism for the inner discharge front at the initial stage (after the second breakdown) and before the development of the pinch effect. The motion of the discharge at this stage is determined by heat conductivity. It occurs in a manner similar to the slow spreading of a laser spark [4, 5] or an hg discharge [6]: As a result of heat conductivity, the energy from the developed breakdown region is transferred to the gas layers located before the discharge front, whereby they are heated until there develops considerable ionization, sufficient for intensive release of Joule heat.

We shall confirm the validity of this mechanism by calculation.

The phenomenon in question must be described in terms of a nonstationary model. This is mostly due to the fact that Joule heat is continuously released behind the discharge front, so that, generally speaking, a steady-state temperature cannot be established itself.

The situation is, however, considerably simplified by the fact that, under our conditions, the time during which the discharge moves through a distance on the order of the discharge front width is short in comparison with the characteristic time of gas temperature variation behind the discharge front. Therefore, the problem of discharge propagation can be solved in a quasistationary approximation, where the temperature behind the discharge front is assumed to be "frozen."

Under our experimental conditions, the width of the discharge front is much smaller than the front curvature radius, which is close to the radius of the tube where the discharge is produced (the difference amounts to more than one order of magnitude). This makes it possible to describe the process within the framework of a two-dimensional model.

Furthermore, since, under these experimental conditions, the width of the discharge ring at the swelling stage, and even more so, the width of the discharge front, is much smaller than the characteristic distance over which the rotational electric field that maintains the discharge varies, we shall subsequently consider that the strength of the electric field is uniform.

Finally, in view of the fact that the characteristic time during which the discharge moves through a distance roughly equal to its front width is much shorter than the characteristic time determining the variation of the electric field, we shall consider that the electric field is constant in time.

The validity of all these assumptions can be checked by using the expressions given at the end of the article.

In describing the discharge stage under consideration, we neglect the effect which the magnetic field exerts on the discharge. This is admissible for the following reasons. As is shown by an analysis of the photographs obtained by means of the SPR, the discharge "swelling" occurs within a time interval during which the strength of the rotational electric field varies near its maximum value, which corresponds to the time $\tau/2$ in

Fig. 2, when intensive release of Joule heat starts in the discharge. During this time interval, the strength of the magnetic field, which is proportional to the current intensity i in the inductor and varies in phase with the latter, either is sufficiently small or vanishes altogether.

We place the coordinate origin at the wall of the discharge vessel with the x axis pointing in the direction of discharge propagation, perpendicular to this wall (Fig. 4), where 1 is the temperature profile and 2 is the wall of the discharge vessel. We use the following system of equations for describing the propagation process:

$$\partial\rho/\partial t + \partial\rho u/\partial x = 0; \tag{3.1}$$

$$\rho(\partial u/\partial t + u\partial u/\partial x) + \partial p/\partial x = 0; \tag{3.2}$$

$$\frac{\partial}{\partial t}\rho\left(\varepsilon+\frac{u^2}{2}\right)+\frac{\partial}{\partial x}\left[\rho u\left(\varepsilon+\frac{p}{\rho}+\frac{u^2}{2}\right)-\lambda\frac{\partial T}{\partial x}\right]=\sigma E^2, \tag{3.3}$$

$$p = \rho kT/M,\ \varepsilon = c_v T,$$

where ρ is the gas density; u, gas velocity; p, pressure; ε, internal energy per unit mass; λ, thermal conductivity coefficient; T, temperature; σ, conductivity; E, strength of the electric field, which is assumed to be uniform in space and constant in time; c_v, specific heat at constant volume; k, Boltzmann constant; and M, atomic mass of the gas. Temperatures $\leqslant$ 10,000°K are considered in the expressions for p and ε.

Let us state the boundary conditions. Ahead of the discharge front ($x=\infty$), the gas temperature and density are assigned: $T(\infty)=T'_0$, $\rho(\infty)=\rho'_0$. For $x=0$, i.e., at the wall of the discharge vessel, the gas velocity vanishes ($u(0)=0$), and discharge propagation occurs in the following manner: As it expands, the heated gas sets in motion the cold gas layers, so that, as a result of thermal conductivity, the discharge now propagates through moving gas. We state the last boundary condition for the temperature on the basis of the assumption that the gas is adiabatically insulated on the side of the discharge tube due to the short duration of the process; i.e., we assume that $-\lambda\partial T(0)/\partial x=0$. In order to complete the statement of the problem, it would be necessary to indicate the initial distributions of the parameters to be determined. However, in the quasistationary approximation used for solving this problem, it is not necessary to know the initial distributions, and we shall not dwell on this question.

We subdivide the region encompassed by the discharge into three zones. In the first zone, which is located to the left of the AA' plane (see Fig. 4), we neglect the role of Joule heat, assuming that the gas is heated here only through thermal conductivity and that intensive release of Joule heat occurs in the region to the right of the AA' plane. If we assume that the conductivity σ is a rather critical function of the temperature (which obtains if the temperatures are not too high), i.e., that a slight drop in T brings about a considerable reduction in σ, the temperature T_1 at the location corresponding to the AA' plane will be obviously not much different from the final temperature T_f for $x=0$, and we can assume that $(T_f-T_1)/T_f \ll 1$. Then, in the region to the right of the AA' plane, we neglect the gas motion and the pressure variation, assuming that $u\approx 0$ and $p\approx$ const. Such an approximation, while greatly simplifying calculations, does not distort substantially the final results. We place the BB' plane in such a way that the change in temperature from T_1 to the final value T_f occurs practically in the second zone, which is located between AA' and BB'. Then, in the third zone, between BB' and the wall of the discharge vessel, the temperature gradient is $\partial T/\partial x\simeq 0$ in correspondence with the boundary condition at $x=0$, so that the heat released in this zone is used up almost entirely on gas heating.

As the discharge propagates, the AA' plane moves in the gas. We assume that the displacement rate of this plane is equal to the discharge velocity. In our experiments, the discharge propagation velocity was determined with respect to the rate of expansion of the region of intensive gas luminescence, which is shown in high contrast in the photographs (see Fig. 3). Since the radiation intensity at temperatures T lower than T_1 ($T_1 \sim 8000$°K) drops extremely sharply with a reduction in T, the temperature pertaining to the inner front of the discharge in Fig. 3a can be only slightly lower than T_1. This indicates the validity of the above definition of the discharge propagation rate as the expansion rate of the region where intensive release of Joule heat takes place. Let us pass to a coordinate system with respect to which the AA' plane is at rest. Since we neglect the gas motion in the zone to the right of the AA' plane in the laboratory coordinate system, then, in a coordinate system where AA' is fixed, the gas velocity D in the region of this plane is equal to the velocity of the AA' plane relative to the wall of the discharge vessel; i.e., it coincides with the discharge propagation rate to be determined. Considering that the temperature T_f at the location corresponding to the BB' plane is assigned, neglecting its variation on the basis of our approximation, and assuming that the thermal flux vanishes at the BB' plane in correspondence with the above, we can investigate in the chosen coordinate system the discharge

structure in the region to the left of BB' in a stationary approximation; i.e., we can neglect the derivatives with respect to time in Eqs. (3.1)-(3.3).

In the first zone, which is located to the left of the AA' plane, assuming that $\sigma \cong 0$, we obtain after integrating the original system of differential equations the following system of algebraic equations for determining the absolute value of D:

$$\rho_0' u_0 = \rho_f D, \quad \frac{\rho_0' k T_0'}{M} + \rho_0' u_0^2 = \frac{\rho_f k T_f}{M} + \rho_k D^2,$$

$$\rho_f D \left[c_p (T_f - T_0') + \left(\frac{D^2}{2} - \frac{u_0^2}{2} \right) \right] = q_1,$$

where ρ_f is the gas density at the temperature T_1 (corresponding to the region where the AA' plane is located), which is approximately equal to T_f according to the relationship $(T_f - T_1)/T_f \ll 1$, u_0 is the gas velocity ahead of the discharge, c_p is the specific heat at constant pressure, and q_1 is the thermal flux which carries away energy from the second zone (between AA' and BB').

Considering the relationships $(T'_0/T_1) \ll 1$, $(u_0/D) = (\rho_f/\rho_0) \ll 1$, and introducing the notation $p'_0 = \rho'_0 k T'_0/M$, we obtain the following equation for determining D:

$$D^3 - 2(q_1/p_0') D^2 + 2c_p T_f D - 2(q_1/p_0')(kT_f/M) = 0. \tag{3.4}$$

In order to calculate q_1, we consider the second zone (between AA' and BB'). As was mentioned above, in view of the critical dependence of σ on T, the gas is heated slightly in this zone: $(T_f - T_1)/T_f \ll 1$. This results in the fact that virtually all of the liberated heat is transferred to the cold gas layers by thermal conductivity, while the role of convection is secondary. Actually, the ratio of the terms describing the conductive and the convective heat removal from the second zone is evidently equal to $\lambda/\rho u c_p \Delta x$ (Δx is the width of the second zone, which is related to the temperature gradient in the region of the AA' plane by the expression $(T_f - T_1)/|dT/dx|$). The value of $\lambda/\rho u c_p$ is approximately equal to the characteristic distance to which the gas is heated in the region ahead of the AA' plane; i.e., it is equal to the width of the first zone, which is related to the temperature gradient in the region of the AA' plane by the expression $(T_1 - T'_0)/|dT/dx|$. Therefore, the above expression for a comparative estimate of the roles of thermal conductivity and convection is equivalent to the relationship $(T_1 - T'_0)/(T_f - T_1) \approx T_f/(T_f - T_1) \gg 1$; i.e., the statement concerning the insignificant effect of convection on the thermal balance in the second zone has been proved correct. Then we write for the second zone

$$\frac{d}{dx} \lambda \frac{dT}{dx} + \sigma E^2 = 0.$$

From this, we find the expression for the thermal flux q_1 by considering the fact that the thermal flux vanishes in the region of the BB' plane, where $T = T_f$:

$$q_1 = \sqrt{2 \int_{T_1}^{T_f} \lambda \sigma E^2 dT} \approx \sqrt{2 \int_{0}^{T_f} \lambda \sigma E^2 dT};$$

in writing the latter (approximate) expression, we have taken into account the fact that the thermal flux is virtually unaffected by the value of the lower integration limit in view of the critical temperature dependence of σ.

By investigating graphically Eq. (3.4), we can satisfy ourselves that $D \sim \sqrt{2 \int_{0}^{T_f} \lambda \sigma E^2 dT} \Big/ p_0'$; i.e., the discharge propagation rate for the assigned pressure p'_0 before the discharge front is described by an expression similar to the Zel'dovich–Frank-Kamenetskii equation [7] for the rate of flame propagation from the closed-off end of a tube.

In order to complete the solution of this problem, it is necessary to determine the gas pressure p'_0 before the discharge front. In the case of subsonic discharge propagation, which has been investigated in [4-6], the value of p'_0 is equal to the undisturbed gas pressure. In our case, the discharge velocity, while remaining lower than the velocity of sound in the heated gas, is at the same time higher than the velocity of sound in the cold gas. The expansion of heated gas occurs at a velocity which is supersonic in relation to the cold gas, and this results in the formation of a shock wave, which propagates ahead of the discharge front as it compresses, heats, and sets in motion the gas located before the front.

In our approach to the solution of the problem of discharge propagation, it is assumed that the shock front is located at infinity, i.e., that its distance from the discharge region is much larger than the width of the discharge front. In view of this, the temperature jump, which determines the position of the shock front, is not marked in Fig. 4; instead, the profile of Fig. 4 describes the temperature distribution in the region behind the shock front. For the same reason, in stating the problem, T'_0 and ρ'_1 at $x=\infty$ are understood as the gas temperature and density that are established immediately behind the shock front, and not the temperature T_0 and the density ρ_0 of the unperturbed gas located before this front. The remoteness of the shock front in the above calculations was used in integrating the energy balance equation, where it was assumed that the thermal flux vanishes ahead of the discharge front (but behind the shock front) at $x=\infty$ ($\partial T/\partial x=0$). The fact that, under the conditions under consideration, the shock front actually moves to a considerable distance (in the above sense) from the discharge front during the time characteristic for the discharge development stage under investigation (which amounts roughly to a quarter of the oscillation period of the inductor current) can be verified by using the expressions for the shock wave velocity and the discharge front width given below.

In view of the condition $(u_0/D) \ll 1$, the velocity of the gas in motion by the shock wave is approximately equal to the discharge propagation velocity D (in the laboratory coordinate system).

By taking into account this fact, assigning the values of ρ_0 and T_0 (or $p_0=\rho_0 kT_0/M$) for the undisturbed gas before the shock front, and considering the laws of conservation of mass, momentum, and energy, which hold at the front of the shock wave, we can, after obtaining the solution, define p'_0 as a function of p_0, ρ_0, and D. By substituting the thus found value of p'_0 in (3.4), we find the velocity D.

Such calculations are generally rather cumbersome. However, they can be simplified by considering the relationship $(p'_0/p_0) \gg 1$. The following equality then holds [8]:

$$p'_0 \simeq p_0 \frac{2\gamma}{\gamma+1}\left(\frac{V}{c_0}\right)^2, \tag{3.5}$$

where γ is the adiabatic exponent, $c_0=\sqrt{\gamma p_0/\rho_0}$ is the velocity of sound in indisturbed gas, and V is the shock wave velocity, which is related to the velocity of the gas set in motion by the shock wave D by the expression

$$V=\frac{\gamma+1}{2}D. \tag{3.6}$$

By substituting (3.5) and (3.6) in (3.4), we obtain for the discharge propagation rate a fifth-power equation with respect to D, which cannot be solved analytically in the general case.

It is convenient to investigate this equation graphically. Analysis shows that it has for D a unique, real, positive solution, whose values are encompassed within a rather narrow interval:

$$\sqrt[3]{4q_1\Big/\left(\frac{2c_pM}{k}\right)(\gamma+1)\rho_0} < D < \sqrt[3]{4q_1/(\gamma+1)\rho_0}\left(\sqrt[3]{\frac{2c_pM}{k}} \approx 1.7\right).$$

With regard to our conditions ($p_0 \sim 30$ mm Hg; $E \sim 70$ V/cm, and $T_f \sim 10{,}000$°K), calculations show that the velocity D is on the order of 1 km/sec, which is in good agreement with the experimental results.

We shall now verify the above-mentioned fact that the gas temperature varies slowly behind the discharge front. The width of the discharge front is defined by two regions: the zone of intensive Joule heat release (the region between AA' and BB' in Fig. 4) and the zone where the gas is heated by the thermal flux, which is located to the left of the AA' plane. As was shown above, the characteristic dimension of the latter zone is much larger than the width of the region located between AA' and BB'. Consequently, the width of the discharge front is virtually equal to the width of the heating zone located to the left of AA' and is, therefore, on the order of $l=\lambda/\rho_f D c_p$. Subsequently, it should be borne in mind that the quantity c_p in the expression for l constitutes the specific heat of cold gas (located before the discharge), while λ corresponds to the temperature value in the region of the AA' plane. This fact is important, since, beginning with temperatures of $\approx$8000°K, the values of c_p and λ increase rather sharply due to the increasing contribution of ionization and electron thermal conductivity, respectively, while the "limiting" temperature T_1 under our conditions ($T_f \approx 10{,}000$°K) is actually close to 8000°K, which can readily be checked by using the corresponding data for the conductivity σ. It should be noted that the thermal diffusivity $\lambda/\rho c_p$ varies relatively slowly.

The characteristic time τ_{fr} during which the discharge moves over a distance roughly equal to the width of its front is equal to l/D. The gas temperature variation behind the front (i.e., in the region to the right of BB' plane), where $p \approx$ const and $\partial T/\partial x \approx 0$, is described by the equation

$$\rho c_p \partial T/\partial t = \sigma E^2 \tag{3.7}$$

(here ρ, c_p, and σ correspond to temperatures close to T_f).

It is evident from (3.7) that, during the short time interval τ_{fr}, the gas temperature behind the discharge front varies by an amount approximately equal to

$$\Delta T \approx \tau_{fr} \sigma E^2/\rho c_p. \tag{3.8}$$

By substituting in (3.8) the above expression for τ_{fr} and the numerical values of all the quantities characterizing the discharge, we satisfy ourselves that the value of ΔT is small in comparison with T_f under these conditions; i.e., the process of discharge propagation can in fact be investigated in a quasistationary approximation.

The authors are grateful to Yu. P. Raizer for a detailed discussion of this paper.

LITERATURE CITED

1. A. F. Aleksandrov and A. A. Rukhadze, Physics of High-Current Electric-Discharge Light Sources [in Russian], Atomizdat, Moscow (1976).
2. S. I. Andreev, O. G. Baikov, and P. N. Dashuk, "Energy loss from an optically thin xenon plasma layer," Teplofiz. Vys. Temp., 8, No. 5 (1970).
3. V. I. Myshenkov and Yu. P. Raizer, "Ionization wave propagation caused by the diffusion of resonance quanta and maintained by shf radiation," Zh. Eksp. Teor. Fiz., 61, No. 5(11) (1971).
4. F. V. Bunkin, V. I. Konov, A. M. Prokhorov, and V. B. Fedorov, "Laser spark under slow burn conditions," Pis'ma Zh. Eksp. Teor. Fiz., 9 (1969).
5. Yu. P. Raizer, "Subsonic propagation of a light spark and threshold conditions for maintaining the plasma by radiation," Zh. Eksp. Teor. Fiz., 58 (1970).
6. Yu. P. Raizer, "Propagation of an shf high-pressure discharge," Zh. Eksp. Teor. Fiz., 61 (1971).
7. D. A. Frank-Kamenetskii, Diffusion and Heat Transfer in Chemical Kinetics, Plenum Publ. (1969).
8. Ya. B. Zel'dovich et al., Physics of Shock Waves and High Temperature Hydrodynamic Phenomena, Academic Press.